

# Time-dependent spectra of quantum beats

Héctor M. Castro-Beltrán<sup>1,\*</sup> and Ricardo Román-Ancheyta<sup>2,†</sup>

<sup>1</sup>*Centro de Investigación en Ingeniería y Ciencias Aplicadas, Universidad Autónoma del Estado de Morelos, Avenida Universidad 1001, 62209 Cuernavaca, Morelos, Mexico*

<sup>2</sup>*Centro de Física Aplicada y Tecnología Avanzada, Universidad Nacional Autónoma de México, Boulevard Juriquilla 3001, 76230 Querétaro, Mexico*

(Dated: December 19, 2024)

We obtain time-resolved spectra of spontaneous emission and resonance fluorescence of a single multilevel emitter where two antiparallel transitions interfere and cause quantum beats. After rising as a single broad peak, the spontaneous emission spectrum turns into a doublet of subnatural peaks and then fades for long times. For strong field resonance fluorescence, the beat signature is the formation of doublet sidebands, which initially grow asymmetrically but end up symmetrical. We stress the filter bandwidth's crucial role in the spectral resolution and causal evolution.

## I. INTRODUCTION

Quantum beats (QB), the modulation of the fluorescence signal of a multilevel system by the interference of two or more close frequencies of transitions from, e.g., the fine or hyperfine structure, are among the more familiar and interesting manifestations of quantum mechanics [1], with applications in high-resolution spectroscopy and quantum technologies [2–12]. Its observation requires ignoring the frequencies of the emitted photons when observed by a broadband detector after the atom (or other emitter) was prepared in a superposition of states. In most quantum beat experiments, light from spontaneous emission is observed, but it can also be from resonance fluorescence after cw laser excitation [13] or other processes [14, 15].

A QB is a time-resolved effect, so its spectrum, the frequencies that compose the beats, is obtained from the Fourier transform of the excited state populations if spontaneous emission is measured or from the stationary dipole correlation function, the Wiener-Khintchine (WK) formula, for resonance fluorescence. Besides being defined differently, these spectra are only snapshots obtained long after the start of the interaction. They do not tell the story of how they reached such spectra. This is problematic for general time-dependent excitation (pulsed, chirped, sudden, constant, etc.) or internal structures, like the one causing the QBs we study here, and other couplings of the emitter.

To address the need for a comprehensive definition of time-dependent spectra (TDS), Eberly and Wódkiewicz (EW) devised the Physical Spectrum [16], based on photon counting at the relevant frequencies [17] and filtering due to the detector's bandwidth [18], intrinsic components of the measurement process that guarantee positivity and compliance with the time-energy uncertainty, acknowledging that one cannot resolve both spectrum and time development arbitrarily at the same time.

In this paper we show theoretically that quantum beat effects can be nicely captured in the EW TDS of spontaneous emission and resonance fluorescence from a single two-level atom with angular momentum  $J = 1/2 - J' = 1/2$ , subject to Zeeman splittings, the beats resulting from interference among the  $\pi$  transitions ( $m = m'$ ) [13].

Interestingly, the time-resolved spontaneous emission spectrum develops from a broad single peak into a doublet, the signature of beats, and then fades away. This fading sounds odd but, after all, there is only one photon to be emitted, after which there is no light and thus no spectrum. And, very importantly, we obtain and provide an exact analytical result.

For stationary resonance fluorescence, if the laser and magnetic fields are strong, the beats have a well-defined mean and modulation frequency in observables such as the intensity and two-time correlation functions [13]. The dipole correlation gives way to a Wiener-Khintchine, Mollow-like spectrum given by a central peak and sidebands that are actually doublets, again, the signature of QBs. In contrast, we show that the time-dependent spectrum evolves asymmetrically with oscillations at the spectral components' frequencies and ends up symmetric.

A Fabry-Perot type of filter has a crucial role in the EW spectra: for once, it selects the frequency component of the emission [18], but it also blurs the order of photon arrivals at the detector, which manifests as linewidth narrowing in the TDS of spontaneous emission [19]. As a consequence, the bandwidth must be chosen so that the doublets are sufficiently resolved, but also that the beating wave packets are not entirely bypassed.

Nonstationary systems have been common subjects of EW TDS. Ideal optical cavities [20–22], anisotropic polaritons [23], quantum thermometers [24], superconducting qubits [25], and oscillating mirrors [26, 27] produce long-term stabilized spectra. Turn-on [19] and turn-off [28] of the atom-laser interaction lead to the birth and death (by spontaneous emission), respectively, of the Mollow triplet spectrum of resonance fluorescence [29]. Even under continuous wave driving, some fluorescence processes have nontrivial TDS under specific conditions, such as initial coherence [30] and coherent population

\* hcastro@uaem.mx

† ancheyta@fata.unam.mx

trapping [31, 32]. Recently, with others, we studied the TDS of blinking resonance fluorescence [33], observing that the Mollow spectrum emerges well before the ultra-narrow peak due to electron shelving [34–36]. TDS of light [16] are of practical interest for emerging applications in quantum optics [37, 38] and quantum control [39, 40], where measurements are constrained by time.

## II. MODEL

The studied system, depicted in Fig. 1 (a), consists of a single two-level emitter with angular momentum states  $|J, m\rangle$ , where  $J = 1/2$  for both levels and  $m = \pm J$  is the magnetic quantum number, giving the upper states  $|1\rangle \equiv |1/2, -1/2\rangle$  and  $|2\rangle \equiv |1/2, 1/2\rangle$ , and the lower states  $|3\rangle \equiv |1/2, -1/2\rangle$  and  $|4\rangle \equiv |1/2, 1/2\rangle$ . This level configuration is found in  $^{198}\text{Hg}^+$  [41] and charged quantum dots [42], for example. We only observe the  $\pi$  transitions ( $m = m'$ ), which have dipole matrix elements  $\mathbf{d}_1 = \langle 1|\hat{\mathbf{d}}|3\rangle = -\mathcal{D}\mathbf{e}_z/\sqrt{3}$ , and  $\mathbf{d}_2 = \langle 2|\hat{\mathbf{d}}|4\rangle = -\mathbf{d}_1$ , where  $\mathcal{D}$  is the reduced dipole matrix element and the sign difference implies that they are antiparallel. The  $\pi$  transitions couple to linearly polarized light along the quantization axis  $z$ .

We remove level degeneracies by the application of a static magnetic field  $B_z$  along the  $z$  direction, the Zeeman effect, with splittings  $g_u\mu_B B_z$  and  $g_\ell\mu_B B_z$  for the upper and lower levels, where  $g_u$  and  $g_\ell$  are the respective Landé  $g$ -factors, and  $\mu_B$  is Bohr's magneton. Thus, the difference Zeeman splitting is  $\delta = (g_u - g_\ell)\mu_B B_z/\hbar$ , so the effective transition frequencies of the  $\pi$  transitions are  $\omega_0 = \omega_{13}$  and  $\omega_{24} = \omega_{13} + \delta$ .

The atom is excited by a monochromatic laser field of frequency  $\omega_L$ , wave vector  $k_L$ , and amplitude  $E_0$ , linearly polarized in the  $z$  direction, propagating in the  $x$  direction,  $\mathbf{E}_L(x, t) = E_0 e^{i(\omega_L t - k_L x)} \mathbf{e}_z + \text{c.c.}$ , driving only the  $\pi$  transitions. The Rabi frequency is then  $\Omega = E_0 \mathcal{D}/\sqrt{3} \hbar$ . The atom-laser detuning is referenced to the  $|1\rangle - |3\rangle$  transition, that is,  $\Delta = \omega_L - \omega_{13}$ , so that  $\Delta - \delta$  is the detuning on the  $|2\rangle - |4\rangle$  transition.

Defining the atomic operators  $A_{jk} = |j\rangle\langle k|$ , where  $j \neq k$  denotes coherences, and  $j = k$  denotes populations, and in the frame rotating at the laser frequency, we finally have the Hamiltonian [43]

$$H = -\hbar\Delta A_{11} - \hbar(\Delta - \delta)A_{22} + \hbar B_z(A_{22} + A_{44}) + \hbar\Omega [(A_{13} - A_{24}) + \text{h.c.}]. \quad (1)$$

The excited states decay by spontaneous emission either in the  $\pi$  transitions, emitting photons with linear polarization at rate  $\gamma_\pi$ , or in the  $\sigma$  transitions, emitting photons with circular polarization at rate  $\gamma_\sigma$ , with branching ratios of 1/3 and 2/3, respectively [43]. The total decay rate of each excited state is then  $\gamma = \gamma_\pi + \gamma_\sigma$ .

The positive-frequency part of the source field operator in the far-field zone is given by [13, 43]

$$\hat{E}_\pi^+(\mathbf{r}, t) = f_\pi(r) [A_{31}(t) - A_{42}(t)] \mathbf{e}_z, \quad (2)$$

where  $f_\pi(r) = -\omega_0^2 \mathcal{D}/4\sqrt{3}r\pi\epsilon_0 c^2$ , is a constant factor we henceforth drop, so the total intensity is given by the expectation values of the excited state populations,

$$I_\pi(\mathbf{r}, t) = \langle \hat{E}_\pi^-(\mathbf{r}, t) \hat{E}_\pi^+(\mathbf{r}, t) \rangle = \langle A_{11}(t) \rangle + \langle A_{22}(t) \rangle. \quad (3)$$

## III. TIME-DEPENDENT SPECTRA

We calculate the TDS of the  $\pi$  transitions using the physical spectrum by Eberly and Wódkiewicz [16, 44], defined as

$$S(\nu, t, \Gamma) = \Gamma \int_{t_0}^t dt_1 \int_{t_0}^t dt_2 e^{-(\Gamma/2 - i\nu)(t-t_1)} \times e^{-(\Gamma/2 + i\nu)(t-t_2)} \langle \hat{E}_\pi^-(t_1) \hat{E}_\pi^+(t_2) \rangle, \quad (4)$$

where  $t$  is the time elapsed since the laser turn-on  $t_0 = 0$ ,  $t_2 - t_1 \equiv \tau \geq 0$  is the time delay between two measurements of the field correlation,  $\nu = \omega - \omega_L$  is the detuning of the laser frequency  $\omega_L$  from the filter's frequency  $\omega$ ,  $\Gamma$  is the filter's bandwidth, and  $\langle \hat{E}_\pi^-(t_1) \hat{E}_\pi^+(t_2) \rangle$  is the dipole correlation function. Inserting Eq. (2) into Eq. (4), noting that  $\langle A_{13}(t_1) A_{42}(t_1 + \tau) \rangle$  and  $\langle A_{24}(t_1) A_{31}(t_1 + \tau) \rangle$  are zero due to initial conditions, we have the spectrum written in terms of the atomic operators,

$$S(\nu, t, \Gamma) = 2\Gamma \text{Re} \int_0^t dt_1 e^{-\Gamma(t-t_1)} \int_0^{t-t_1} d\tau e^{(\Gamma/2 - i\nu)\tau} \times [\langle A_{13}(t_1) A_{31}(t_1 + \tau) \rangle + \langle A_{24}(t_1) A_{42}(t_1 + \tau) \rangle] \quad (5)$$

For a stationary process ( $t \rightarrow \infty$ ) and unrealistic perfect resolution ( $\Gamma \rightarrow 0$ ), we recover the Wiener-Khintchine (WK) spectrum,  $S_{\text{WK}}(\nu) = \text{Re} \int_0^\infty d\tau e^{-i\nu\tau} \langle \hat{E}_\pi^-(0) \hat{E}_\pi^+(\tau) \rangle$  [16, 18]. Often a finite detection bandwidth is added phenomenologically, with the replacement  $\nu \rightarrow \nu + i\Gamma$  [43]. The WK spectrum implies a long measurement time, missing whatever changes a spectrum has undergone.

Now, we focus on our results, presenting the technicalities of the analytical and numerical calculations in Appendix A. For QBs to be observable in the system, the primary conditions are that we break the level degeneracy,  $\delta \neq 0$ , and set the initial state in a superposition of both excited states for spontaneous emission or both ground states for resonance fluorescence [13].

A major result of this work is that we obtained the EW TDS of spontaneous emission analytically,

$$S_{\text{SE}}(\nu, t, \Gamma) = \frac{F(t, 0)}{(\gamma - \Gamma)^2 + 4\nu^2} + \frac{F(t, \delta)}{(\gamma - \Gamma)^2 + 4(\nu + \delta)^2}, \quad (6)$$

$$F(t, x) \equiv 2\Gamma (e^{-\Gamma t} + e^{-\gamma t}) - 4\Gamma e^{-\frac{1}{2}(\gamma + \Gamma)t} \cos((\nu + x)t).$$

Figure 1(b) shows a sequence of traces of the time-dependent spontaneous emission spectrum. Initially, for times  $t \sim 1/\Gamma$ , the spectrum is not fully developed, given by a single peak; this is in the filter's filling time. Then,

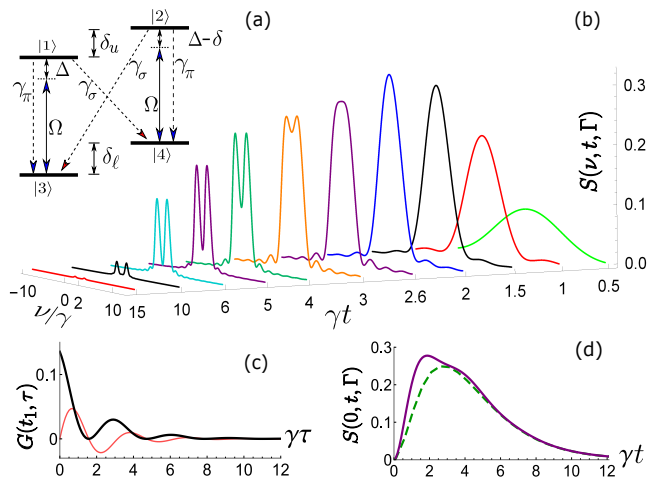


FIG. 1. (a) Atom-laser system (see main text for details). (b) TDS  $S(\nu, t, \Gamma)$  of spontaneous emission, where  $\Omega = \Delta = 0$ , for  $\delta = -2\gamma$ ,  $\Gamma = \gamma/2$ , and initial condition  $\langle A_{11}(0) \rangle = \langle A_{22}(0) \rangle = 1/2$ , with the other  $\langle A_{jk}(0) \rangle = 0$ . (c) Real (black-thick) and imaginary (red-thin) parts of the correlation  $G(t_1, \tau) = \langle \hat{E}_\pi^-(t_1) \hat{E}_\pi^+(t_1 + \tau) \rangle$ ; see Fig. 1(c). In the degenerate case ( $\delta = 0$ ), the spectrum Eq. (6), lacking quantum beats, is reduced to a single peak [19], which grows more slowly than any peak of the doublet, as seen in Fig. 1(d). But what might seem surprising is that the doublet fades for times  $t \gg 1/\Gamma$ . The explanation is simple: the atom emits only one photon. At long times, it is very likely that the atom has already done so, and, eventually, there would be no light in the filter to be transmitted to the detector.

the spectrum splits and becomes a doublet: the peak at  $\nu = 0$  comes from the transition  $|1\rangle \rightarrow |3\rangle$ , while the peak at  $\nu = -\delta = 2$  comes from the transition  $|2\rangle \rightarrow |4\rangle$ . The separation  $|\delta|$  is the modulation (beat) frequency of the decay of the correlation  $G(t_1, \tau) = \langle \hat{E}_\pi^-(t_1) \hat{E}_\pi^+(t_1 + \tau) \rangle$ ; see Fig. 1(c). In the degenerate case ( $\delta = 0$ ), the spectrum Eq. (6), lacking quantum beats, is reduced to a single peak [19], which grows more slowly than any peak of the doublet, as seen in Fig. 1(d). But what might seem surprising is that the doublet fades for times  $t \gg 1/\Gamma$ . The explanation is simple: the atom emits only one photon. At long times, it is very likely that the atom has already done so, and, eventually, there would be no light in the filter to be transmitted to the detector.

We have chosen a filter bandwidth,  $\Gamma = |\delta|/4$ , narrow enough to resolve the doublet but wide enough to fill the filter rapidly and allow for the spectrum to reveal its shape not long after  $t \sim \Gamma^{-1}$ , a manifestation of the time-energy uncertainty. With a very narrow bandwidth,  $\Gamma \ll |\delta|$ , it would take a long time to reveal the final spectral shape, not capturing the QB signature. A large bandwidth,  $\Gamma > |\delta|$ , would give, if anything, a short-lived single-peak spectrum; the broadband regime  $\Gamma \gg |\delta|$  is that of time-resolved beats. Thus, it takes time to measure a spectrum, but our goal is to capture spectral transients by taking only a finite time for the measurement.

Another remarkable effect is the subnatural width of the peaks,  $\gamma - \Gamma$ , a signature of interference of the source light with the filter, which causes uncertainty in the time of arrival and transmission of photons. In the extreme narrowing case,  $\Gamma = \gamma$ , the spectrum Eq. (6) is reduced to  $S_{SE}(\nu, t, \Gamma) = \frac{1}{2} \Gamma t^2 e^{-\Gamma t} \{ \text{sinc}^2(\nu t/2) + \text{sinc}^2[(\nu + \delta)t/2] \}$ , where  $\text{sinc}(z) \equiv \sin(z)/z$ . The peak frequencies ( $\nu =$

0 and  $\nu = -\delta$ ) grow and die as  $\frac{1}{2} \Gamma t^2 e^{-\Gamma t}$ , while their widths are proportional to  $t^{-1}$ , i.e., for  $\Gamma = \gamma$ ,  $S_{SE}(\nu, t, \Gamma)$  evolves into two Dirac delta functions but with vanishing amplitude. The lateral lobes (zeros) of  $\text{sinc}(z)$  explain the small bottom oscillations in the TDS of Fig. 1(b).

Recall that spontaneous emission is a transient process, so it does not have a Wiener-Khinchine spectrum. Conveniently, its spectrum has been defined as the Fourier transform of the upper state population, not of the dipole correlation. A more formal approach [45] is to do a double integral of the dipole correlation,  $P(\nu) \propto \int_0^T dt_1 \int_0^T dt_2 e^{-i\nu(t_1 - t_2)} G(t_1, t_2)$ , still with perfect resolution, obtaining the expected two Lorentzians centered at  $\nu = 0$  and  $\nu = -\delta$  in the long-time limit. These definitions may be useful but miss entirely spontaneous emission's intrinsic transient, single-photon nature.

Now we consider the contrasting case of resonance fluorescence by a highly nondegenerate atomic system driven by a strong laser field,  $\Omega \sim \delta \gg \gamma$  (we choose, for simplicity, resonant excitation,  $\Delta = 0$ ). Fig. 2(a) shows the full spectrum at a short time  $\gamma t = 4$  (left), when it has not fully developed yet, and at a long time  $\gamma t = 15$  (right), very near its stationary shape. It is a Mollow-type spectrum with sidebands that are doublets with peaks of unequal heights at frequencies [13, 43]

$$\Omega_1 = \sqrt{4\Omega^2 + \Delta^2}, \quad \Omega_2 = \sqrt{4\Omega^2 + (\delta - \Delta)^2}. \quad (7)$$

We zoom in on the evolution of the left sideband and

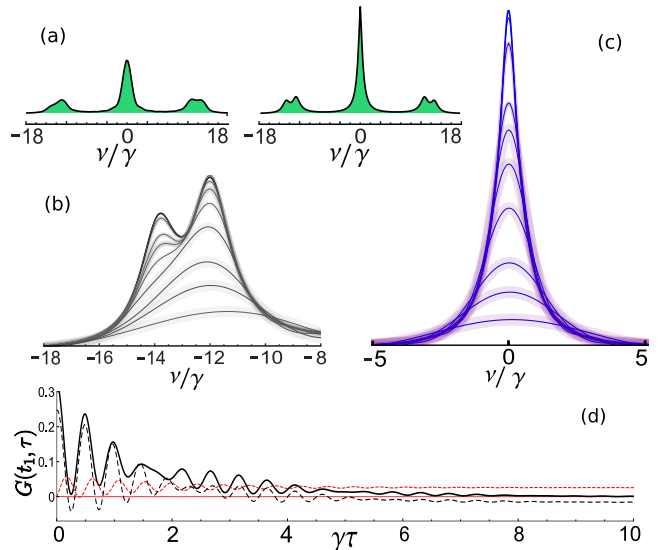


FIG. 2. (a) Full spectrum  $S(\nu, t, \Gamma)$  at short,  $\gamma t = 4$  (left), and long  $\gamma t = 15$  (right), times. Growth of the left sideband (b) and central band (c) at the increasing measurement times  $\gamma t = 1, 3/2, 2, 3, 4, 5, 6, 10, 15, 20$  (lower to higher traces). (d) Dipole correlation  $G(t_1, \tau)$  for  $\gamma t_1 = 1$  (dashed) and  $\gamma t_1 = 7$  (solid), real part (thick) and imaginary (thin). The other parameters are:  $\Omega = 6\gamma$ ,  $\delta = -7\gamma$ ,  $\Delta = 0$ , and  $\Gamma = 0.5\gamma \simeq \Omega_{\text{beat}}/2$ . The initial condition is  $\langle A_{33}(0) \rangle = \langle A_{44}(0) \rangle = 1/2$ , and the other  $\langle A_{jk}(0) \rangle = 0$ .

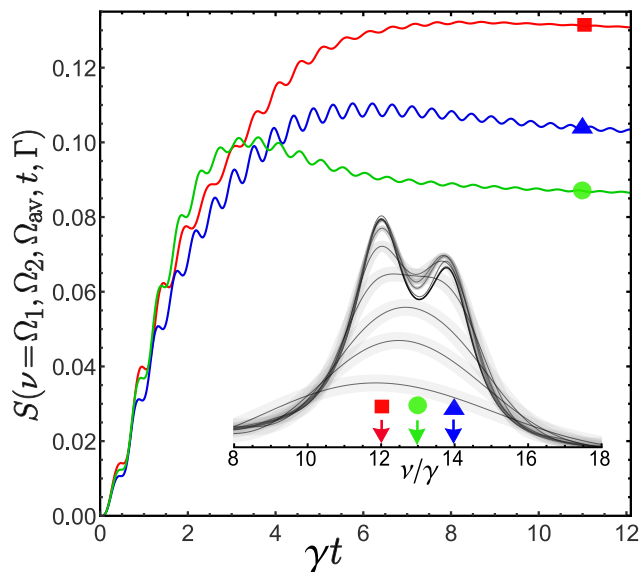


FIG. 3. Evolution of the right doublet sideband of  $S(\nu, t, \Gamma)$  (gray lines) and at the frequencies of the peaks at  $\nu = \Omega_1$  (square) and  $\nu = \Omega_2$  (triangle), and of the dip at  $\nu = \Omega_{av}$  (circle). Other labeling and parameters are as in Fig. 2.

central band in Figs. 2(b,c), and of the right sideband in the inset of Fig. 3, from an early measurement time,  $\gamma t = 1$ , up to a long time,  $\gamma t = 20$ . Comparing the right and left sidebands, we see that the spectrum evolves strongly asymmetrically but eventually reaches a symmetric shape. The transient asymmetry is due to nonzero detunings, here only  $\delta$ . [Fig. 4 of Ref. [33] shows a similar transient asymmetry.] The peaks at  $|\Omega_1| = 12\gamma$  stabilize a little sooner than those at  $|\Omega_2| \simeq 13.9\gamma$  because the  $|1\rangle - |3\rangle$  transition frequency is closer to the laser frequency. The small oscillations in the evolution at the frequencies of the right sideband peaks and the dip, Fig. 3, missing in the steady state, are also due to the detuning.

The features of the spectrum are, of course, related to the properties of the source dipole correlation  $G(t_1, \tau)$ . Most important is that the doublet sidebands result from beats with well-defined mean,  $\Omega_{av} = \frac{1}{2}(\Omega_2 + \Omega_1)$ , and modulation frequency,  $\Omega_{beat} = \frac{1}{2}(\Omega_2 - \Omega_1)$ . These beats occur only in the nondegenerate case ( $\delta \neq 0$ ), where the two  $\pi$  transitions are unbalanced, evolving with Rabi frequencies  $\Omega_1$  and  $\Omega_2$  [13]. Fig. 2(d) shows  $G(t_1, \tau)$  for  $\gamma t_1 = 1$ , which generates the lowest (first trace) spectrum, and  $\gamma t_1 = 7$ , a time long enough to see any further changes and the doublets are already well-formed. Detunings give the correlation a transient nonzero imaginary part (when the spectrum is asymmetric) that vanishes in the steady state.

Again, our choice of the filter bandwidth,  $\Gamma = \gamma/2 \simeq \Omega_{beat}/2$ , is made on the grounds of not only resolving the doublet,  $\Gamma < \Omega_2 - \Omega_1$ , but also capturing the sideband oscillations and beat modulation in  $G(t_1, \tau)$  at times  $t \sim \Gamma^{-1}$ . With a narrower  $\Gamma$ , not only do we miss the

beat and make the oscillations smaller, but the whole spectrum would evolve more symmetrically and monotonically (See Fig. 4 in Appendix B). Causality would prevent the formation of the doublet before the beat occurs. We cannot measure quantum interference before interference occurs. This effect is analogous to the nonobservation of the Rabi doublet in cavity QED before a Rabi oscillation is completed [22].

The nondegenerate  $J = 1/2 - J' = 1/2$  system is relatively simple yet nontrivial that shows quantum interference to several orders of coherence functions. Because the  $\pi$  transitions are antiparallel, that is, they do not end nor start in common states, one would not expect quantum beats in the intensity; they have to be looked at in fluctuations [6–8, 13–15], like the dipole correlation in this work. Still, there are beats in the intensity of resonance fluorescence. The point is that there is an underlying coherence in the scattering due to the initial state preparation for spontaneous emission and the laser for resonance fluorescence, which allows for interference in higher-order functions such as intensity-intensity and intensity-amplitude correlations [13].

An interesting application of the EW Physical Spectrum consists of correlating photons of selected spectrum components [47, 48]. But this comes with the difficulty of handling sets of time-ordered integrals for every photon sequence. There are theoretical and experimental efforts to get around the complications due to filtering (see the review [49] and also [50, 51]), especially for resonance fluorescence in cavity QED. It would be very interesting to study frequency-selected photon correlations from the spectrum of quantum beats. However, this is beyond the purpose of this work.

#### IV. CONCLUSIONS

We have calculated time-dependent spectra of spontaneous emission and resonance fluorescence (pillars of quantum optics) of a system that features quantum beats using the Eberly-Wódkiewicz physical spectrum. The resolution of temporal features in the spectra crucially depends on the bandwidth of the detection technique. Our results show that the richness of behavior of time-dependent spectra can be revealed beyond what is possible with the Wiener-Khinchine spectrum. With this work, we hope to stimulate further studies of time-resolved spectra for stationary and nonstationary systems for a variety of applications, and fundamental questions in quantum mechanics, such as causality and complementarity.

#### V. ACKNOWLEDGMENTS.

H.M.C.-B. thanks Programa de Movilidad Nacional UAEM-UNAM, Convenio No. 42467-2177-8-IX-15, for support to perform part of his work in CFATA. R.R.-

A. thanks DGAPA-UNAM, México for support under Project No. IA104624.

### Appendix A: Master Equation and Quantum Regression Formula

The dynamics of the atom-laser-reservoir system are described by the master equation for the reduced atomic density operator,  $\rho$ . In a frame rotating at the laser frequency this is  $\partial_t \tilde{\rho} = -\frac{i}{\hbar}[H, \tilde{\rho}] + \mathcal{L}_\gamma \tilde{\rho}$ , where  $-\frac{i}{\hbar}[H, \tilde{\rho}]$  describes the coherent atom-laser interaction and  $\mathcal{L}_\gamma \tilde{\rho}$  the damping due to spontaneous emission [43, 46],  $\mathcal{L}_\gamma \tilde{\rho} = \frac{1}{2} \sum_{i,j=1}^2 \gamma_{ij} (2S_i^- \tilde{\rho} S_j^+ - S_i^+ S_j^- \tilde{\rho} - \tilde{\rho} S_i^+ S_j^-) + \frac{\gamma_\sigma}{2} \sum_{i=3}^4 (2S_i^- \tilde{\rho} S_i^+ - S_i^+ S_i^- \tilde{\rho} - \tilde{\rho} S_i^+ S_i^-)$ , where  $S_1^- = A_{31}$ ,  $S_2^- = A_{42}$ ,  $S_3^- = A_{32}$ , and  $S_4^- = A_{41}$ . Noting that the coherences for the  $|1\rangle - |4\rangle$ ,  $|2\rangle - |3\rangle$ ,  $|1\rangle - |2\rangle$ , and  $|3\rangle - |4\rangle$  transitions vanish at all times thus, instead of 16 equations, we are left with a set of 8 relevant homogeneous equations [13]:

$$\begin{aligned} \langle \dot{A}_{11} \rangle &= -\gamma \langle A_{11} \rangle + i\Omega(\langle A_{31} \rangle - \langle A_{13} \rangle), \\ \langle \dot{A}_{13} \rangle &= -\left(\frac{\gamma}{2} + i\Delta\right) \langle A_{13} \rangle - i\Omega(\langle A_{11} \rangle - \langle A_{33} \rangle), \\ \langle \dot{A}_{22} \rangle &= -\gamma \langle A_{22} \rangle - i\Omega(\langle A_{42} \rangle - \langle A_{24} \rangle), \\ \langle \dot{A}_{24} \rangle &= -\left(\frac{\gamma}{2} + i(\Delta - \delta)\right) \langle A_{24} \rangle + i\Omega(\langle A_{22} \rangle - \langle A_{44} \rangle), \\ \langle \dot{A}_{31} \rangle &= -\left(\frac{\gamma}{2} - i\Delta\right) \langle A_{31} \rangle + i\Omega(\langle A_{11} \rangle - \langle A_{33} \rangle), \\ \langle \dot{A}_{33} \rangle &= \gamma_1 \langle A_{11} \rangle + \gamma_\sigma \langle A_{22} \rangle - i\Omega(\langle A_{31} \rangle - \langle A_{13} \rangle), \\ \langle \dot{A}_{42} \rangle &= -\left(\frac{\gamma}{2} - i(\Delta - \delta)\right) \langle A_{42} \rangle - i\Omega(\langle A_{22} \rangle - \langle A_{44} \rangle), \\ \langle \dot{A}_{44} \rangle &= \gamma_\sigma \langle A_{11} \rangle + \gamma_2 \langle A_{22} \rangle + i\Omega(\langle A_{42} \rangle - \langle A_{24} \rangle). \end{aligned} \quad (\text{A1})$$

This then lets us define a simpler Bloch vector  $\mathbf{Q} \equiv (A_{11}, A_{13}, A_{22}, A_{24}, A_{31}, A_{33}, A_{42}, A_{44})^T$ . A set of homogeneous equations translates into a great reduction in numerical calculations compared to the inhomogeneous case, obtained by eliminating, e.g., the population  $\langle A_{44} \rangle$  via the conservation of probability. The resulting Bloch equations for the atomic expectation values can be written compactly as  $\partial_t \langle \mathbf{Q}(t) \rangle = \mathbf{M} \langle \mathbf{Q}(t) \rangle$ , where  $\mathbf{M}$  is an  $8 \times 8$  matrix of coefficients [13] and the formal solution is given by  $\langle \mathbf{Q}(t) \rangle = e^{\mathbf{M}t} \langle \mathbf{Q}(0) \rangle$ .

The advantage of solving only eight homogeneous equations carries over to the two-time correlations. For this, we apply the quantum regression formula [45], that is,  $\partial_\tau \langle \mathbf{W}(t_1, \tau) \rangle = \mathbf{M} \langle \mathbf{W}(t_1, \tau) \rangle$ , where we defined a Bloch-like vector  $\mathbf{W}(t_1, \tau) = A_{jk}(t_1) \mathbf{Q}(t_1 + \tau)$ , and has the formal solution  $\langle \mathbf{W}(t_1, \tau) \rangle = e^{\mathbf{M}\tau} \langle \mathbf{W}(t_1, 0) \rangle$ . We define the two-time operator functions  $\mathbf{U}(t_1, \tau) = A_{13}(t_1) \mathbf{Q}(t_1 + \tau)$  and  $\mathbf{V}(t_1, \tau) = A_{24}(t_1) \mathbf{Q}(t_1 + \tau)$ , from which the second and seventh terms, respectively, are the correlations given in the second line of Eq. (5). Their ex-

pectation values have initial conditions (at  $\tau = 0$ ):

$$\langle \mathbf{U}(t_1, 0) \rangle = (0, 0, 0, 0, \langle A_{11}(t_1) \rangle, \langle A_{13}(t_1) \rangle, 0, 0)^T \quad (\text{A2a})$$

$$\langle \mathbf{V}(t_1, 0) \rangle = (0, 0, 0, 0, 0, 0, \langle A_{22}(t_1) \rangle, \langle A_{24}(t_1) \rangle)^T \quad (\text{A2b})$$

To observe beats in spontaneous emission,  $\Omega = \Delta = 0$ , we need a nonzero difference of Zeeman detunings,  $\delta \neq 0$ , and both upper states must be initially nonzero, ideally equal [13], so the initial Bloch vector is

$$\langle \mathbf{Q}(0) \rangle_{\text{SE}} = (1/2, 0, 1/2, 0, 0, 0, 0, 0)^T. \quad (\text{A3})$$

In this case, we solve the Bloch equations (A1) analytically:  $\langle A_{11}(t) \rangle = \langle A_{22}(t) \rangle = \frac{1}{2} e^{-\gamma t}$ ,  $\langle A_{33}(t) \rangle = \langle A_{44}(t) \rangle = \frac{1}{2} (1 - e^{-\gamma t})$ , with vanishing coherences. Note that the intensity,  $I_\pi^{SE} = e^{-\gamma t}$  [Eq. (3)], shows no quantum beats, so we have to go to the dipole correlation to observe them. Using the quantum regression formula, we get

$$\langle A_{13}(t_1) A_{31}(t_1 + \tau) \rangle = \frac{1}{2} e^{-\gamma\tau/2} e^{-\gamma t_1}, \quad (\text{A4a})$$

$$\langle A_{24}(t_1) A_{42}(t_1 + \tau) \rangle = \frac{1}{2} e^{-(\gamma/2 + i\delta)\tau} e^{-\gamma t_1}. \quad (\text{A4b})$$

Inserting Eqs. (A4) into Eq. (5) gives us the spectrum Eq. (6). For numerical calculations, the populations and coherences are obtained from

$$\langle A_{11}(t) \rangle = ([e^{\mathbf{M}t}]_{11} + [e^{\mathbf{M}t}]_{13})/2, \quad (\text{A5a})$$

$$\langle A_{22}(t) \rangle = ([e^{\mathbf{M}t}]_{31} + [e^{\mathbf{M}t}]_{33})/2, \quad (\text{A5b})$$

$$\langle A_{13}(t) \rangle = ([e^{\mathbf{M}t}]_{21} + [e^{\mathbf{M}t}]_{23})/2 = 0, \quad (\text{A5c})$$

$$\langle A_{24}(t) \rangle = ([e^{\mathbf{M}t}]_{41} + [e^{\mathbf{M}t}]_{43})/2 = 0, \quad (\text{A5d})$$

where the subindices indicate the row and column of the matrix in brackets.

To observe beats in resonance fluorescence, besides  $\delta \neq 0$ , we need both ground state populations to be nonzero initially, optimally

$$\langle \mathbf{Q}(0) \rangle_{\text{RF}} = (0, 0, 0, 0, 0, 1/2, 0, 1/2)^T. \quad (\text{A6})$$

The populations and coherences are:

$$\langle A_{11}(t) \rangle = ([e^{\mathbf{M}t}]_{16} + [e^{\mathbf{M}t}]_{18})/2, \quad (\text{A7a})$$

$$\langle A_{22}(t) \rangle = ([e^{\mathbf{M}t}]_{36} + [e^{\mathbf{M}t}]_{38})/2, \quad (\text{A7b})$$

$$\langle A_{13}(t) \rangle = ([e^{\mathbf{M}t}]_{26} + [e^{\mathbf{M}t}]_{28})/2, \quad (\text{A7c})$$

$$\langle A_{24}(t) \rangle = ([e^{\mathbf{M}t}]_{46} + [e^{\mathbf{M}t}]_{48})/2, \quad (\text{A7d})$$

giving the intensity, Eq. (3),  $2I_\pi^{\text{RF}}(t) = [e^{\mathbf{M}t}]_{16} + [e^{\mathbf{M}t}]_{18} + [e^{\mathbf{M}t}]_{36} + [e^{\mathbf{M}t}]_{38}$ , displayed in Figs. 4 and 5 of Ref. [13].

Following the procedure outlined above, the correlations are

$$\langle A_{13}(t_1) A_{31}(t_1 + \tau) \rangle = [e^{\mathbf{M}\tau}]_{55} \langle A_{11}(t_1) \rangle + [e^{\mathbf{M}\tau}]_{56} \langle A_{13}(t_1) \rangle, \quad (\text{A8a})$$

$$\langle A_{24}(t_1) A_{42}(t_1 + \tau) \rangle = [e^{\mathbf{M}\tau}]_{77} \langle A_{22}(t_1) \rangle + [e^{\mathbf{M}\tau}]_{78} \langle A_{24}(t_1) \rangle, \quad (\text{A8b})$$

where Eqs. (A7) (Eqs. (A5) for spontaneous emission) are to be used, and then integrated as prescribed in Eq. (5) to find the spectrum

$$S(\nu, t, \Gamma) = 2\Gamma \text{Re} \int_0^t dt_1 e^{-\Gamma(t-t_1)} \int_0^{t-t_1} d\tau e^{(\Gamma/2-i\nu)\tau} \\ \times \left\{ [e^{\mathbf{M}\tau}]_{55} \langle A_{11}(t_1) \rangle + [e^{\mathbf{M}\tau}]_{56} \langle A_{13}(t_1) \rangle \right. \\ \left. + [e^{\mathbf{M}\tau}]_{77} \langle A_{22}(t_1) \rangle + [e^{\mathbf{M}\tau}]_{78} \langle A_{24}(t_1) \rangle \right\}. \quad (\text{A9})$$

We want to point to the temporal factorization of the functions of  $t_1$  and  $\tau$  in the correlations Eqs. (A4) and (A8), permitting great simplification of the analytical and numerical evaluations of TDS. This observation allows to suggest the scalability to larger multilevel systems [7] as long as the Bloch equations are homogeneous. Otherwise, the computations might be much more involved.

To ensure the reproducibility of our results for the reader's benefit, we share our source code in [52].

### Appendix B: Effect of Narrower and Broader Filter Bandwidth

Figure 4 shows the sidebands in the TDS of quantum beats in resonance fluorescence for finer ( $\Gamma = 0.1\gamma$ , top panel) and coarser ( $\Gamma = \gamma$ , lower panel) filter resolution

than those of Figs. 2 and 3. The spectrum evolves more symmetrically with finer filter resolution, and the dip is better resolved. With a coarser filter, the asymmetry persists longer and the dip becomes shallow.

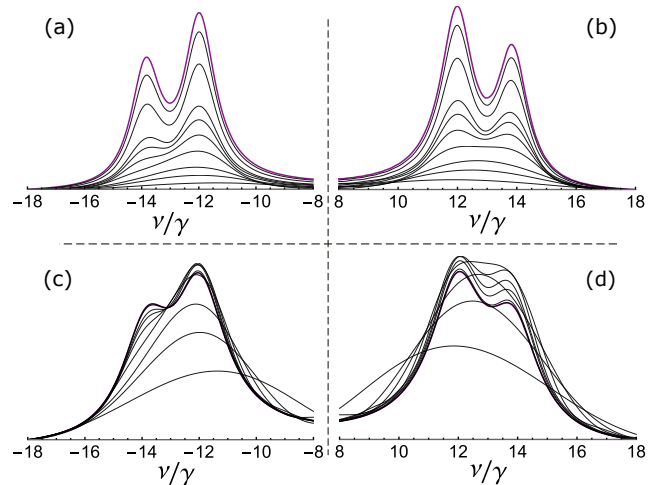


FIG. 4. Evolution of the left (left panel) and right (right panel) doublet sidebands of  $S(\nu, t, \Gamma)$ . Same parameters as Figs. 2 and 3 except for  $\Gamma = 0.1\gamma$  for (a) and (b), and  $\Gamma = \gamma$  for (c) and (d). The purple (thicker) solid line is the trace at  $\gamma t = 20$ , i.e., very close to the steady state.

- 
- [1] G. Breit, Quantum Theory of Dispersion (Continued). Parts VI and VII, *Rev. Mod. Phys.* **5**, 91 (1933).
  - [2] S. Haroche, Quantum beats and time-resolved fluorescence spectroscopy, in *High-Resolution Laser Spectroscopy*, K. Shimoda, ed. (Springer, Berlin, 1976).
  - [3] E. Hack and J. R. Huber, Quantum beat spectroscopy of molecules, *International Reviews in Physical Chemistry*, **10**, 287 (1991).
  - [4] S. B. Bayram, P. Arndt, O. I. Popov, C. Güney, W. P. Boyle, M. D. Havey, and J. McFarland, Quantum beat spectroscopy: Stimulated emission probe of hyperfine quantum beats in the atomic Cs  $8p^2P_{3/2}$  level, *Phys. Rev. A* **90**, 062510 (2014).
  - [5] A. C. LaForge, A. Benediktovitch, V. Sukharnikov, *et al*, Time-resolved quantum beats in the fluorescence of helium resonantly excited by XUV radiation, *J. Phys. B: At. Mol. Opt. Phys.* **53**, 244012 (2020).
  - [6] A. Zajonc, Proposed quantum-beats: Quantum-eraser experiment, *Phys. Lett.* **96A**, 61 (1983).
  - [7] D. G. Norris, L. A. Orozco, P. Barberis-Blostein, and H. J. Carmichael, Observation of ground-state quantum beats in atomic spontaneous emission, *Phys. Rev. Lett.* **105**, 123602 (2010).
  - [8] A. D. Cimmarusti, C. A. Schroeder, B. D. Patterson, L. A. Orozco, P. Barberis-Blostein, and H. J. Carmichael, Control of conditional quantum beats in cavity QED: amplitude decoherence and phase shifts, *New J. Phys.* **15**, 013017 (2013).
  - [9] A. V. Trifonov, A. S. Kurdyubov, I. Ya. Gerlovin, D. S. Smirnov, K. V. Kavokin, I. A. Yugova, M. Aßmann, and A. V. Kavokin, Exciton energy oscillations induced by quantum beats, *Phys. Rev. B*, **102**, 205303 (2020).
  - [10] R. Cai, I. Wadgaonkar, J. W. M. Lim, S. Dal Forno, D. Giovanni, M. Feng, S. Ye, M. Battiato, and T. Chien Sum, Zero-field quantum beats and spin decoherence mechanisms in CsPbBr<sub>3</sub> perovskite nanocrystals, *Nat. Commun.* **14**, 2472 (2023).
  - [11] A. Lee, H. S. Han, F. K. Fatemi, S. L. Rolston, and K. Sinha, Collective quantum beats from distant multilevel emitters, *Phys. Rev. A* **107**, 013701 (2023).
  - [12] Z. Wu, J. Li, and Y. Wu, Vacuum-induced quantum-beat-enabled photon antibunching, *Phys. Rev. A* **108**, 023727 (2023).
  - [13] H. M. Castro-Beltrán, O. de los Santos-Sánchez, L. Gutiérrez, and A. D. Alcantar-Vidal, Quantum interference in the resonance fluorescence of a  $J = 1/2 - J' = 1/2$  atomic system: Quantum beats, nonclassicality, and non-Gaussianity, *Phys. Rev. A* **109**, 013702 (2024).
  - [14] Z. Ficek and S. Swain, *Quantum Interference and Coherence: Theory and Experiments* (Springer, New York, 2005).
  - [15] R. Yano, H. Shinojima, K. Nakagawa, Quantum beats in fluorescence for multi-level atomic system, *Appl. Surf. Sci.*, **255**, 9585 (2009).
  - [16] J. H. Eberly and K. Wódkiewicz, The time-dependent physical spectrum of light, *J. Opt. Soc. Am.* **67**, 1252 (1977).

- [17] L. Mandel and E. Wolf, *Optical Coherence and Quantum Optics* (Cambridge University Press, Cambridge, 1995).
- [18] M. Born and E. Wolf, *Principles of Optics, 7th ed.* (Cambridge University Press, Cambridge, 1999).
- [19] J. H. Eberly, C. V. Kunasz, and K. Wódkiewicz, Time-dependent spectrum of resonance fluorescence, *J. Phys. B: Atom. Molec. Phys.* **13**, 217 (1980).
- [20] J. J. Sanchez-Mondragon, N. B. Narozhny, and J. H. Eberly, Theory of spontaneous-emission line shape in an ideal cavity, *Phys. Rev. Lett* **51**, 550 (1983); erratum *Phys. Rev. Lett* **51**, 1925 (1983).
- [21] H. M. Castro-Beltran, S. M. Chumakov, and J. J. Sanchez-Mondragon, Collective-resonance fluorescence in an ideal cavity, *Phys. Rev. A* **53**, 4420 (1996).
- [22] M. Yamaguchi, A. Lyasota, T. Yuge, and Y. Ota, Time-resolved physical spectrum in cavity quantum electrodynamics, *Phys. Research* **4**, 023052 (2022).
- [23] M. Salado-Mejía, R. Román-Ancheyta, F. Soto-Eguibar, and H. M. Moya-Cessa, Spectroscopy and critical quantum thermometry in the ultrastrong coupling regime, *Quantum Sci. Technol.* **6** 025010 (2021).
- [24] R. Román-Ancheyta, B. Çakmak, and Ö. E. Müstecaplıoğlu, Spectral signatures of non-thermal baths in quantum thermalization, *Quantum Sci. Technol.* **5** 015003 (2020).
- [25] O. de los Santos-Sánchez and R. Román-Ancheyta, Strain-spectroscopy of strongly interacting defects in superconducting qubits, *Supercond. Sci. Technol.* **35** 035005 (2022).
- [26] A. W. Glaetzle, K. Hammerer, A. J. Daley, R. Blatt, and P. Zoller, A single trapped atom in front of an oscillating mirror, *Opt. Commun.* **283**, 758 (2010).
- [27] I. M. Mirza, Real-time emission spectrum of a hybrid atom-optomechanical cavity, *J. Opt. Soc. Am. B* **32**, 1604 (2015).
- [28] X. Y. Huang, R. Tanaś, and J. H. Eberly, Delayed spectrum of two-level resonance fluorescence, *Phys. Rev. A* **26**, 892 (1982).
- [29] B. R. Mollow, Power spectrum of light scattered by two-level systems, *Phys. Rev.* **188**, 1969 (1969).
- [30] J. E. Golub and T. W. Mossberg, Transient spectra of strong-field resonance fluorescence, *Phys. Rev. Lett.* **59**, 2149 (1987).
- [31] A. S. Jayarao, S. V. Lawande, and R. D'Souza, Time-dependent spectra of a strongly driven three-level atom, *Phys. Rev. A* **39**, 3464 (1989).
- [32] A. Mishra and B. N. Jagatap, Time dependent fluorescence spectrum of a three-level  $\Lambda$  system under electromagnetically induced transparency and coherent population trapping, *J. Mod. Optics* **70**, 920 (2024).
- [33] R. Román-Ancheyta, O. de los Santos-Sánchez, L. Horvath, and H. M. Castro-Beltrán, Time-dependent spectra of a three-level atom in the presence of electron shelving, *Phys. Rev. A* **98**, 013820 (2018).
- [34] V. Bühner and Chr. Tamm, Resonance fluorescence spectrum of a trapped ion undergoing quantum jumps, *Phys. Rev. A* **61**, 061801 (2000).
- [35] J. Evers and Ch. H. Keitel, Narrow spectral feature in resonance fluorescence with a single monochromatic laser field, *Phys. Rev. A* **65**, 033813 (2002).
- [36] H. M. Castro-Beltrán, R. Román-Ancheyta, and L. Gutiérrez, Phase-dependent fluctuations of intermittent resonance fluorescence, *Phys. Rev. A* **93**, 033801 (2016).
- [37] S. J. van Enk, Time-dependent spectrum of a single photon and its positive-operator-valued measure, *Phys. Rev. A* **96**, 033834 (2017).
- [38] L. Horvath and Z. Ficek, Initial-phase spectroscopy as a control of entangled systems, *J. Phys. B: At. Mol. Opt. Phys.* **43**, 125506 (2010).
- [39] D. Guéry-Odelin, A. Ruschhaupt, A. Kiely, E. Torrontegui, S. Martínez-Garaot, and J. G. Muga, Shortcuts to adiabaticity: Concepts, methods, and applications, *Rev. Mod. Phys.* **91**, 045001 (2019).
- [40] R. R. Ancheyta, Vacuum radiation versus shortcuts to adiabaticity, *Phys. Rev. A* **108**, 022217 (2023).
- [41] D. Polder and M. F. H. Schuurmans, Resonance fluorescence from a  $j = 1/2$  to  $j = 1/2$  transition, *Phys. Rev. A* **14**, 1468 (1976).
- [42] M. V. G. Dutt, J. Cheng, Bo Li, X. Xu, X. Li, P. R. Berman, D. G. Steel, A. S. Bracker, D. Gammon, S. E. Economou, R.-B. Liu, and L. J. Sham, Stimulated and spontaneous optical generation of electron spin coherence in charged GaAs quantum dots, *Phys. Rev. Lett.* **94**, 227403 (2005).
- [43] M. Kiffner, J. Evers, and C. H. Keitel, Interference in the resonance fluorescence of two incoherently coupled transitions, *Phys. Rev. A* **73**, 063814 (2006).
- [44] H. J. Carmichael, *Statistical Methods in Quantum Optics 2: Non-Classical Fields* (Springer-Verlag, Berlin, 2008).
- [45] H. J. Carmichael, *Statistical Methods in Quantum Optics 1: Master Equations and Fokker-Planck Equations* (Springer-Verlag, Berlin, 2002).
- [46] G. S. Agarwal, *Quantum Statistical Theories of Spontaneous Emission and their Relation to Other Approaches* (Springer-Verlag, Berlin, 1974).
- [47] G. Nienhuis, Spectral correlations in resonance fluorescence, *Phys. Rev. A* **47**, 510 (1993).
- [48] G. Nienhuis, Spectral correlations within the fluorescence triplet, *Europhysics Letters* **21** 285 (1993).
- [49] E. Zubizarreta Casalengua, J. C. López Carreño, F. P. Laussy, and E. del Valle, Conventional and unconventional photon statistics, *Laser Photon. Rev.* **14**, 1900279 (2020).
- [50] J. Ngaha, S. Parkins, and H.J. Carmichael, Multimode array filtering of resonance fluorescence, *Phys. Rev. A* **110**, 023719 (2024).
- [51] H. M. Castro-Beltran, S. M. Chumakov, and J. J. Sanchez-Mondragon, Photon correlations in the spectrum of a superradiant system in a strong cavity field, *Phys. Rev. A* **57**, 1458 (1998).
- [52] H. M. Castro-Beltrán and R. Román-Ancheyta, Time-Dependent Spectra of Quantum Beats, Zenodo (2024), <https://doi.org/10.5281/zenodo.14042889>.